Investigating Space Radiation Environment Effects on Communication of Razaksat-1

Wayan Suparta[1], Siti Katrina Zulkeple[2]

Suparta W http://orcid.org/0000-0002-6193-1867

Zulkeple SK https://orcid.org/0000-0001-9356-4523

ABSTRACT: This study attempted to identify whether space radiation sources could have affected the communication on RazakSAT-1 that was orbiting in a Low Earth Orbit-Near Equatorial (LEO-NEqO). Data on galactic cosmic rays (GCR), trapped protons, trapped electrons, and solar energetic particles (SEPs) obtained from Space Environment Information System (SPENVIS) are considered. The effects of these radiation sources are analyzed using the linear energy transfer (LET), total ionizing dose (TID), and solar cell degradation. Flux data from National Oceanic and Atmospheric Administration (NOAA) 15, 16, and 17 satellites, and the geomagnetic conditions during the time when RazakSAT-1's missing is also analyzed. Another two satellites, Satélite de Coleta de Dados (SCD-2) and Advanced Land Observation Satellite (ALOS), are compared with the performance of RazakSAT-1. Results showed that GCR dominated at a high energy range of 10^3 MeV and above in the LEO-NEqO, whereas the energies of the trapped protons and trapped electrons are less than 400 MeV and 4 MeV, respectively. There are no SEPs estimated during the mission period (2009 – 2011). Based on the SPENVIS, SCD-2 and ALOS are more exposed to higher radiation damage than RazakSAT-1. Thus, an analysis of space radiation environment effects on the RazakSAT-1 communication lost after one year of operation will be discussed further, as a platform to find the best strategy for future missions.

KEYWORDS: Low earth orbit, Linear energy transfer, Total ionizing dose, Non-ionizing energy loss.

INTRODUCTION

RazakSAT-1, which was launched in 2009, is Malaysia's second remote sensing satellite after TiungSAT-1 satellite (Ahmad 2013). The satellite was designed to operate in a low earth orbit (LEO) and near-equatorial orbit (NEqO) at an altitude of 685 km with 9° of inclination. This orbital position allows for a satellite revisit frequency of 90 min, which is more frequent than a sun-synchronous orbital satellite. At this altitude, RazakSAT-1 can monitor the equatorial environment. The payload in RazakSAT-1 was designed with a medium-sized aperture camera (MAC) and five linear detectors, each of which consists of one panchromatic band and four multispectral bands that are designed to capture high-resolution images (Hashim *et al.* 2013). The high-resolution images contribute to Malaysia's development by aiding land management, resource development and forestry. The satellite's high-speed transmission system can download 32 Gb of stored image data within 3 – 4 daytime passes (Chun *et al.* 2006). Power is supplied by solar cells made of GaAs/Ge, whereas the battery uses NiCd. Overall, RazakSAT-1 had a positive outlook. However, the mission was uncompleted after one year in the orbit. The true cause of uncompleted mission was unknown due to unavailability of the vehicle telemetry. This study was motivated by this situation with aim to verify whether space radiation environment of LEO-NEqO had a role in affecting the mission.

To analyze the distribution of space radiation environment such as trapped particles, a Space Environment Information System (SPENVIS) tool is used (Heynderickx *et al.* 2004). This system includes the NASA AP-8 and AE-8 models. Samwell and Hady (2009) has used the models in the SPENVIS to forecast the 2012 space environment for the newly launched EGYPTSAT-2 satellite to assist the satellite team in proper planning decisions. EGYPTSAT-2 is a LEO satellite that orbits the polar region. They predicted that for a 1.5 mm aluminum (Al) shielding thickness, a minimum of total ionizing dose (TID) of 2.65×10^4 rads through the silicon (Si) material and a displacement damage dose (DDD) of 7.75×10^7 MeV/g (Si) to be provided for a five-year mission. Lawal and Radice (2013) has suggested a new satellite system to provide a near 24-hour data in the equator region by using a Synthetic Aperture Radar (SAR) satellite. However, studies on the space environment using this system have not been reported.

In this paper, space radiation, i.e., galactic cosmic ray (GCR), trapped particles, and solar energetic particles (SEPs), in the LEO-NEqO as a plausible cause of uncompleted mission of RazakSAT-1 using the SPENVIS online tool is examined. The orbital data of RazakSAT-1 is compared with the higher inclination of the Satélite de Coleta de Dados (SCD-2) and the polar Advanced Land Observation Satellite (ALOS). In addition, this work provides additional information on the natural characteristics of the LEO-NEqO environment. To support the analysis, the geomagnetic conditions and added the National Oceanic and Atmospheric Administration / Polar Operating Environmental Satellites (NOAA/POES) data for comparison is also examined.

METHODOLOGY
ESTIMATING FLUXES

The models used to predict the space environment of the LEO-NEqO are shown in Fig. 1. These models are available in SPENVIS, which is an online tool that contains many integrated models designed for various simulation-based studies (Heynderickx *et al.* 2004). All of these models were run for magnetic storms to provide the worst-case scenario. From the figure, the fluxes of GCR, SEP, trapped protons, and trapped electrons in the RazakSAT-1 satellite orbit are firstly estimated. The orbit of RazakSAT-1 was set at 9° of inclination with a perigee of 662 km and an apogee of 687 km for the three-year mission from July 14, 2009 to
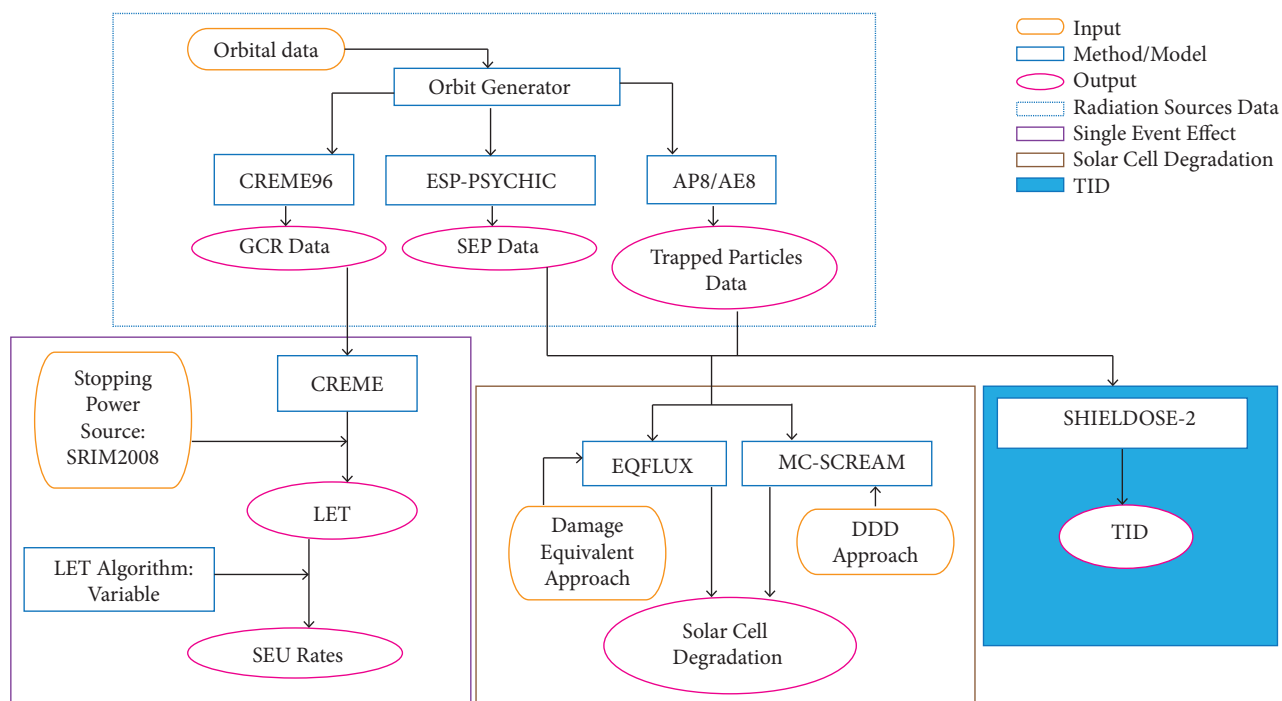

Figure 1. Block diagram of the procedures used in SPENVIS to predict the space radiation environment for the three-year mission (2009 – 2012).

July 14, 2012. Two satellites, i.e., SCD-2 and ALOS, are compared with the performance of RazakSAT-1. SCD-2 is a data-collection satellite from Brazil under the program of the Instituto Nacional de Pesquisas Espaciais (National Institute of Space Research or INPE), whereas ALOS is an earth observation satellite developed by the Japan Aerospace Exploration Agency (JAXA). Orbital data on these satellites are simplified in Table 1. Both RazakSAT-1 and SCD-2 satellites are located in NEqO, whereas ALOS is located in a polar orbit. Therefore, different inclinations can be compared.

Table 1. Orbital data of three satellites: two in NEqO and one in the polar orbit.

Satellite	NEqO Orbit Razaksat-1	NEqO Orbit SCD-2	Polar Orbit ALOS
Perigee (km)	662	743	691
Apogee (km)	687	768	693
Inclination (degree)	9	25	98.16

To generate GCR fluxes, the CREME96 model is used because it includes anomalous cosmic ray (ACR) and low-energy components that are not available in other models. ACR are partially ionized particles with low energy that can be trapped in the earth's inner radiation belt due to its single-charge nature. In addition, CREME96 utilizes the solar minimum data from 1977 to estimate the GCR fluxes. Four available GCR models in SPENVIS (ISO 15390, CREME86, CREME96, and Nymmik) are also compared to identify their abilities to generate GCR fluxes in NEqO and polar orbits. The ESP-PSYCHIC (Xapsos *et al.* 2007) model is used to estimate long-term SEP flux fluence over the three years. This model is useful because its data are taken from various satellites in three solar cycles, which allowed the model to predict a wide range of energy, from 1 MeV to above 100 MeV. SEPs are estimated during a solar maximum and a magnetic storm.

Finally, the established of NASA AP-8 and AE-8 models are selected to generate fluxes of trapped protons and trapped electrons, respectively. AP-8 can cover an energy range of 0.1 to 400 MeV for trapped protons (Sawyer and Vette 1976) and AE-8 can cover an energy range of 0.04 to 7 MeV for trapped electrons (Vette 1991). In this study, the trapped particles are estimated during a solar minimum that follows the period of the mission of RazakSAT-1. Then, the fluxes are applied to calculate the radiation doses.

RADIATION DOSE CALCULATION

The effects of space radiation are described as single-event effects (SEEs) and cumulative effects. SEE used linear energy transfer (LET) parameters and the cumulative effects used TID parameters. The solar cell degradation, which involved a type of cumulative effect called non-ionizing energy loss (NIEL), is included in the calculation.

The LET spectrum inside the spacecraft is derived from differential energies that are generated from the models. The differential energy *f(E)* inside the spacecraft is converted into the differential LET *f(S)* using the CRÈME method (Adams Jr. 1986):

$$f(S) = f(E) \, dE/dS \tag{1}$$

The differential energy *f(E)* is defined as:

$$f(E) = f'(E') \left| \frac{S(E')}{S(E)} \right|^{-\sigma t} \tag{2}$$

where: *f'(E')* is the differential energy at the outer shell of the spacecraft, *S(E')* and *S(E)* are the stopping powers of the ions with energies *E'* and *E*, respectively, and *t* is the thickness of the spacecraft in g/cm^2 of Al or equivalent Al, and σ is defined as:

$$\sigma = \frac{\left[5 \times 10^{-26} A_g \left(A_n^{1/3} + 27^{1/3} - 0.4 \right)^2 \right]}{27} \tag{3}$$

where: A_g is Avogadro's number and A_n is the atomic mass of the incident ion.

The LET spectrum is used to determine the single-event upset (SEU). SEU is a soft error that commonly occurs in the electronics of orbiting spacecraft. Since different energies can produce similar LETs, the variable LET algorithms are fed into the calculation to determine the upset rate (U) and defined as:

$$U = \pi A \sum_{z=1}^{92} \left[\int_{p_{min}}^{p_{max}} D(p) \int_{E_0}^{E_{max}} F(E,Z) dE dp \right] \tag{4}$$

where: A is the surface area of the sensitive volume, $D(p)$ is the differential path-length distribution in the sensitive volume (cm^2g^{-1}), and $F(E,Z)$ is the differential ion energy flux ($m^{-2}sr^{-1}s^{-1}MeV^{-1}$). In addition to Eq. 4, p_{min} is the minimum path length for depositing the minimum energy to cause an upset, as such, only energy above the minimum energy can cause an upset, and E_{max} corresponds to the maximum energy in the ion spectrum.

By applying the Eqs. 1 to 4 through SPENVIS, LET and SEU rates are determined in a gallium arsenide (GaAs) device, which was shielded with 5 mm Al. Then, the LET and SEU rates in the orbits of RazakSAT-1, SCD-2, and ALOS are compared. In SPENVIS, a computer code called SHIELDOSE is used to determine the radiation dose as a function of depth in a shielded material (Seltzer 1994). However, the upgraded version called SHIELDOSE-2 is used to calculate the TID because it better represents proton nuclear interactions and includes more choices of target materials (Barkas and Berger 1964). The target materials are GaAs and Si. When incident particles hit geometric shapes, they are calculated differently. Electrons are calculated with the Monte Carlo code ETRAN, which considered the Bremsstrahlung effect. The doses are estimated for different orbital data of RazakSAT-1, SCD-2 and ALOS over three years.

Apart from that, solar cell degradation is estimated using EQFLUX (Tada *et al.* 1982) and MC-SCREAM (Messenger *et al.* 2008) programs. EQFLUX uses the damage-equivalent approach with 1 MeV electron fluence in the selected orbit. MC-SCREAM uses the DDD method, which applies the NIEL parameter to estimate the end-of-life (EOD). For both programs, the degradation of the GaAs material that was shielded with various cover-glass thicknesses is estimated. GaAs was selected because it was the material of the solar cell in RazakSAT-1. Then, the solar cell degradation in three orbital datasets of RazakSAT-1, SCD-2, and ALOS for the three-year period is compared.

GEOMAGNETIC CONDITIONS

To evaluate the geomagnetic conditions during the approximate period of RazakSAT-1 failure, the trapped particle fluxes were taken from the Medium Energy Proton and Electron Detector (MEPED) sensors onboard three NOAA/POES satellites (NOAA-15, 16, and 17) with geomagnetic indices of K_p and Dst (disturbance storm time) compared. Data are obtained from NOAA website. In this study, omnidirectional proton channels, which are free from data contamination, is used (Rodger *et al.* 2010). The energy channels that were used are simplified in Table 2. Both K_p and Dst indices are obtained from the International Service of Geomagnetic Indices (ISGI). The evaluation of the geomagnetic conditions is set to three months (June to August, 2010).

Table 2. NOAA/POES data energy channels for omnidirectional proton channels.

Data Channels	Abbreviation of Data Channels	Energy Range (MeV)
P6 omni	mepomp6	> 16
P7 omni	mepomp7	> 35
P8 omni	mepomp8	> 70
P9 omni	mepomp9	> 140

RESULTS AND DISCUSSION
FLUX ANALYSIS

Figure 2 displays the space particles present in LEO-NEqO, where RazakSAT-1 is represented by the LEO-NEqO. The figure compares GCR with trapped protons (Fig. 2a), GCR with trapped electrons (Fig. 2b) and finally, between the two trapped particles (Fig. 2c). Based on the figure, trapped particles in LEO-NEqO decrease with energy while GCR flux is peaked at 10^4 GeV. Moreover, the peak values for the maximum energies of GCR, trapped proton, and trapped electron during RazakSAT-1 mission period are approximately 4.8 $m^{-2} s^{-1} s^{-1}$, 60.3 $cm^{-2} s^{-1}$, and 1.6 $cm^{-2} s^{-1}$, respectively. This shows that LEO/NEqO contains GCR with high energy that ranges from 5 GeV to 20 GeV, trapped protons with an energy between 0.1 MeV to 400 MeV, and trapped electrons with an energy of 0.04 MeV to 4 MeV. GCR have lower fluxes than trapped particles and trapped protons for energy < 3 MeV. The lower GCR fluxes are due to the fact that most of the incoming GCR have been attenuated by the Earth's magnetic field while the inner radiation belt, particularly the South Atlantic Anomaly (SAA), are already in LEO/NEqO and it contributes to the trapped particles population. Hence, based on the peak values estimated in LEO/NEqO, the orbit consist of 91% trapped protons, 2% trapped electrons, and 7% GCR.
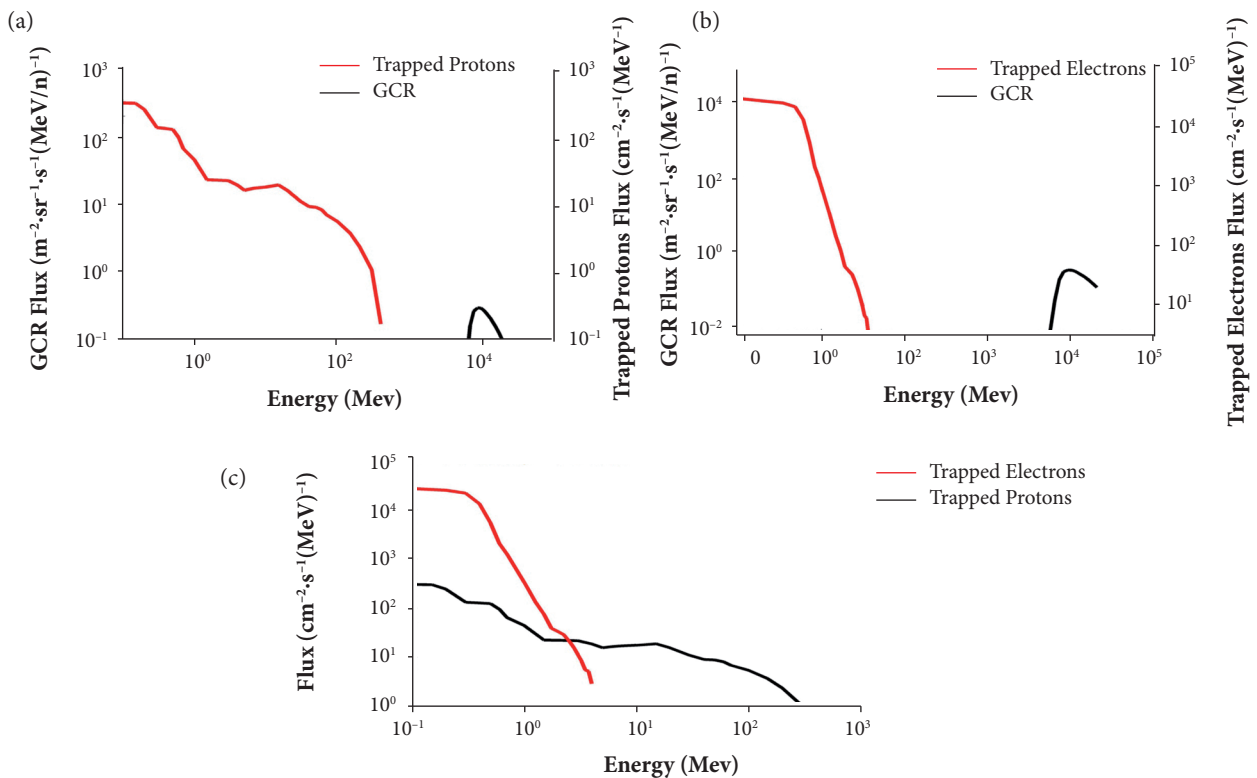

Figure 2. Comparison of (a) GCR and trapped protons, (b) GCR and trapped electrons, and (c) trapped protons and trapped electrons in LEO/NEqO.

SEPs, on the other hand, are not estimated in LEO/NEqO because the SPENVIS models were unable to detect the values, which indicates that the particles are deflected by the geomagnetic cutoff near the equator. However, SEPs can be estimated at higher inclination, which indicates that SEPs have a greater chance of reaching the earth's poles than the equator when large fluences are involved (Benton and Benton 2001). Low-energy SEPs are more common in LEO than high-energy SEPs.

Comparison of trapped protons, trapped electrons, and GCR among the three satellites can be seen in Fig. 3. Here, RazakSAT-1 received the lowest flux because of its low inclination as compared to the other two satellites. The fluxes of trapped protons in RazakSAT-1 (Fig. 3a) can differ by approximately 8 to 10 times with SCD-2 and 100 times with ALOS. Furthermore, for trapped
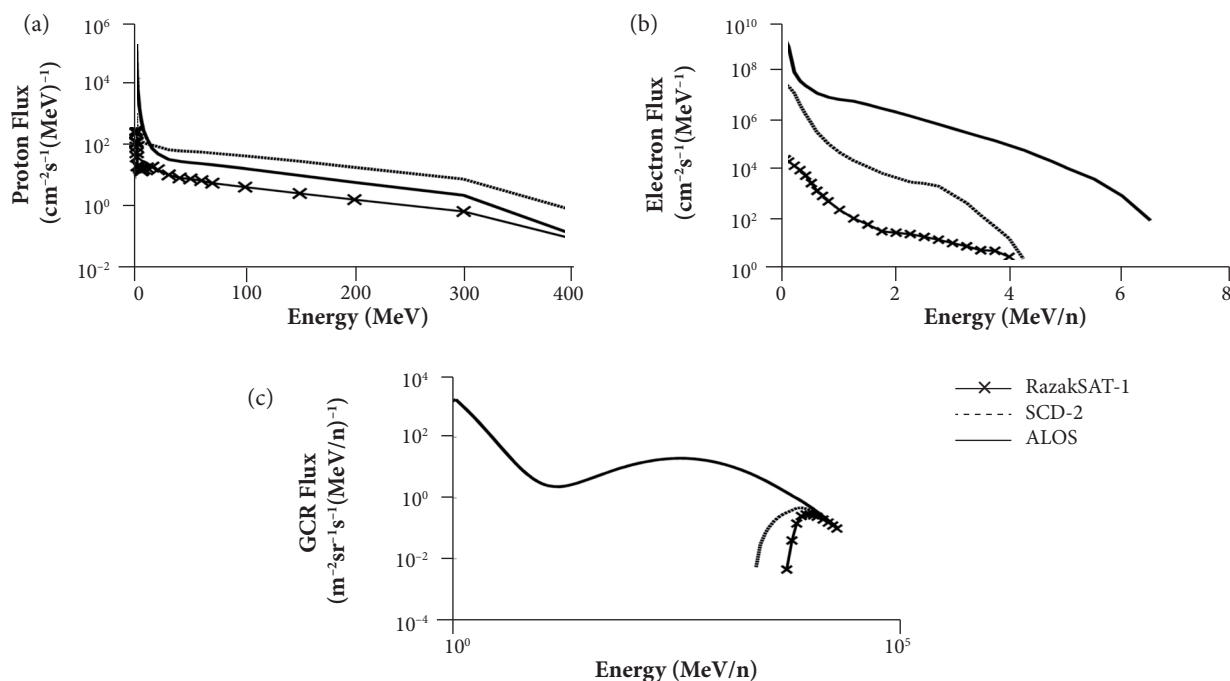
Figure 3. Comparison between three orbital satellites for fluxes of (a) trapped protons, (b) trapped electrons, and (c) GCR.

electrons (Fig. 3b), the flux in RazakSAT-1 can differ up to 650 and 1,000 times from those of SCD-2 and ALOS, respectively. Moreover, the maximum estimated energy range for trapped electrons in NEqO is 4 MeV and can increase to 6 MeV for polar orbits. For GCR (Fig. 3c), it has energy above 5×10^3 MeV, which is 75% lower as compared to polar orbit. Moreover, the GCR fluxes in the orbits of SCD-2 and ALOS are 1.70 and 16.23 times higher, respectively as compared to that of RazakSAT-1. The model indicates that SCD-2 and ALOS are more exposed to GCR particles than RazakSAT-1 because of their higher inclinations.

RADIATION DOSE ANALYSIS

The level of radiation damage towards the three satellites can be explained using the LET, TID, and solar cell parameters. Figure 4 shows the LET results caused by the major space particles in LEO/NEqO (Fig. 4a) and the comparison of LET results between three satellite orbits (Fig. 4b). By referring to Fig. 4a, trapped particles are mostly responsible for the lower LET while GCR is the sole contributor for higher LET in LEO/NEqO. However, RazakSAT-1 in LEO/NEqO was estimated to have the lowest LET damage (the maximum LET was 1,087 MeV cm^2 g^{-1}) as compared to SCD-2 and ALOS (Fig. 4b), where all three satellite orbits demonstrated a decrease of spectra with increasing LET. For a 5 mm shielding, the estimated overall LET fluences of RazakSAT-1 were 1.3 to 9.4 times less than those of SCD-2 and approximately 3 to 120 times less than those of ALOS.

The predicted SEU rates in a 5 mm Al-shielded GaAs of the three satellites are shown in Table 3. RazakSAT-1 was estimated to have the lowest probability of SEU events compared with the other satellites. In fact, a 5 mm Al shielding can reduce the SEU rates by 2.70% for RazakSAT-1. However, SCD-2 demonstrates the highest SEU rates because of its frequent visits over the SAA, where exposure of proton is higher.

Although LET depends on the particle type and energy, it is used to predict the effect of a single event as a result of particle interactions with the target material. The effects include direct ionization and proton-induced ionization. Through LET, the protons directly interact with the target materials to cause ionization. Proton-induced ionization or nuclear interactions occur when the protons transfer energy to the target nucleus, which results in recoil particles that contribute to further ionization. These two mechanisms lead to SEU events. In some cases, increasing the shielding results in the formation of secondary particles where nuclear interactions will significantly multiply these secondary
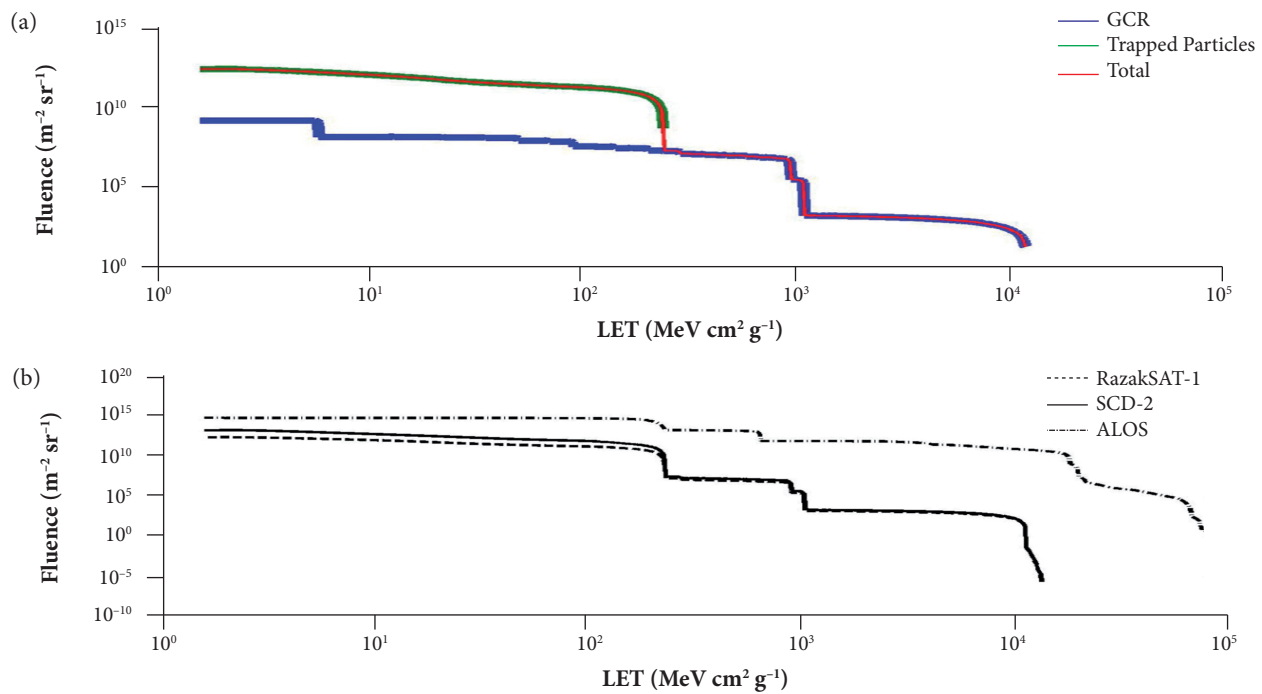
Figure 4. LET spectra for (a) the major space particles in RazakSAT-1 and (b) through GaAs shielded with 5 mm Al for three satellites over three years.

Table 3. SEU rates in 5 mm Al shielded GaAs for three satellites.

Effect/Satellite	Razaksat-1	SCD-2	ALOS
Direct Ionization (bit^{-1})	2.13×10^{-2}	3.52×10^{-2}	1.89×10^{-1}
Proton-Induced Ionization (bit^{-1})	6.48×10^{-2}	6.54×10^{-1}	2.70×10^{-1}
Total Ionization (bit^{-1})	8.61×10^{-2}	6.89×10^{-1}	4.59×10^{-1}

particles, and finally, increase the dose. This scenario appears to occur for all three satellites. Therefore, ionization by nuclear interactions is greater than direct ionization. Thus, protons are the major contributor to the ionization effect in the GaAs device, as opposed to heavy ions.

For the TID analysis, Fig. 5a shows the dose-depth curve of the GaAs material as a result of interacting with trapped protons of RazakSAT-1 during a solar minimum. Based on the figure, three types of radiation are estimated for the total dose of electrons, Bremsstrahlung radiation, and trapped protons. The dose can be reduced by increasing the shielding thickness. However, increasing the shielding by approximately 4 mm or more is not significant for trapped protons. In fact, more shielding is less effective and increases construction costs issues in space designs (Murtaza 2011), and the electrons do not contribute significantly to Bremsstrahlung particles as their curve decreases. Meanwhile, Fig. 5b shows the dose comparison among the three satellites and the highest dose is found for ALOS. With 5 mm shielding, the estimated total TID received by RazakSAT-1 is 2.30×10^2 rads, which is 50% lower than the estimated dose in SCD-2 and ALOS. The dose-depth curve is found to flatten above 4 mm and 10 mm for SCD-2 and ALOS, respectively, which further implies that thicker shielding becomes less effective in reducing the dose.

For materials used in spacecraft, the dose comparison Si and GaAs is compiled in Table 4. Here, Si material exhibited a higher dose of 34% as compared to the GaAs material, which shows that the GaAs material is expected to have better resistance against radiation damage than the Si material in designing the shielding of a spacecraft.
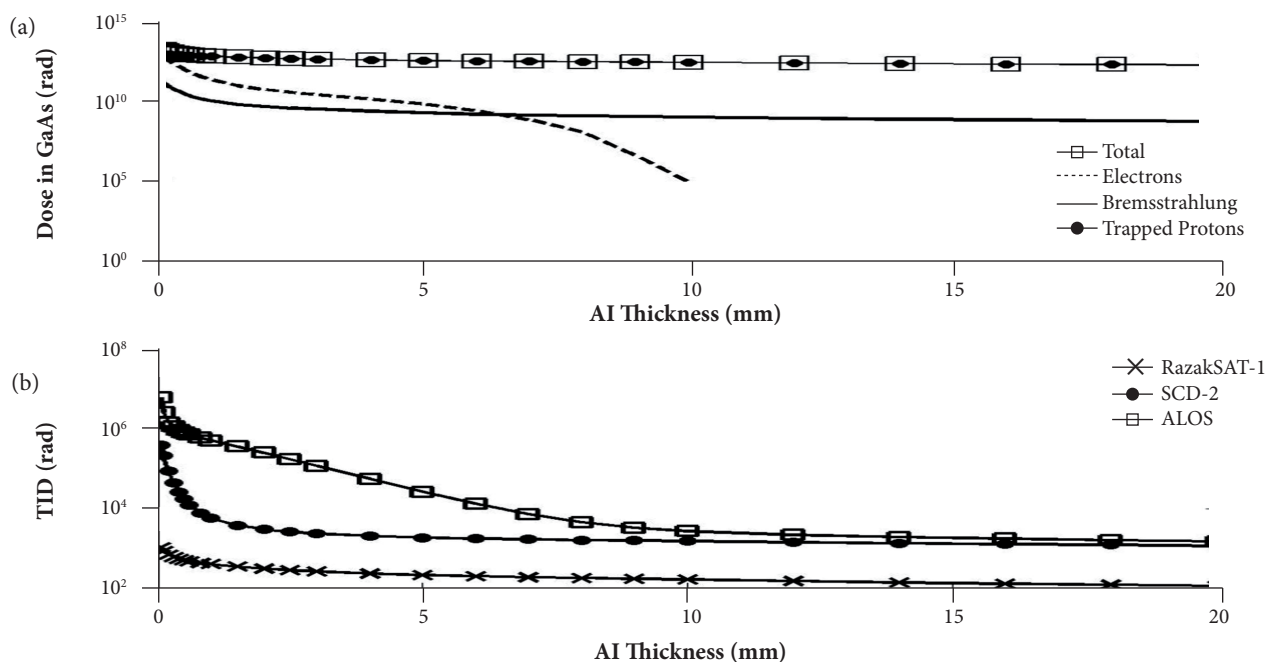
Figure 5. TID in (a) LEO/NEqO and in (b) three satellites based on GaAs material for a period of three years.

Table 4. Absorbed dose of two materials shielded by selected thickness in NEqO for three years.

Al Thickness (mm)	Total TID (rad)	
	GaAs	Si
1	4.29×10^2	5.84×10^2
2	3.32×10^2	4.47×10^2
3	2.82×10^2	3.77×10^2
4	2.52×10^2	3.35×10^2
5	2.30×10^2	3.05×10^2
6	2.16×10^2	2.86×10^2

For GaAs solar cells, the effective dose of 1 MeV electrons as a function of the shielding thickness in the three satellite orbits is presented in Fig. 6. Similar to other doses, the increase in the cover-glass thickness reduces the radiation damage to solar cells. Among the three satellites, RazakSAT-1 and ALOS solar cells received the lowest and highest dose, respectively. The performance of the solar cells is based on the maximum power capability and the influence of the silica glass thickness. This characteristic is demonstrated using the GaAs material as shown in Fig. 7a. Based on this figure, the damage to the solar cells on the three satellites can be reduced by more than 50% with the use of 0.1 mm silica glass. However, the shield thickness above 0.2 mm for both RazakSAT-1 and SCD-2 and above 0.5 mm for ALOS will not reduce the radiation dose, although their doses continue to slowly decrease. Comparing the three satellites, the solar cells in RazakSAT-1 are expected to attain the highest power capability during the three-year mission, followed by SCD-2 and ALOS. In the RazakSAT-1, a very thin silica glass (~ 0.01 mm) is required to protect its solar cells. Increasing the cover-glass thickness does not significantly change the outcome. For the other two satellites, the 0.01 mm silica glass can increase the performance of SCD-2 and ALOS by 0.40% and 2.19%, respectively. RazakSAT-1 can perform 0.57% and 2.62% better than SCD-2 and ALOS, respectively. Meanwhile, Fig. 7b shows a comparison of the degradation of GaAs with the Si material in the RazakSAT-1 orbit. Similar to Fig. 7a, the power of the solar cells can be improved by
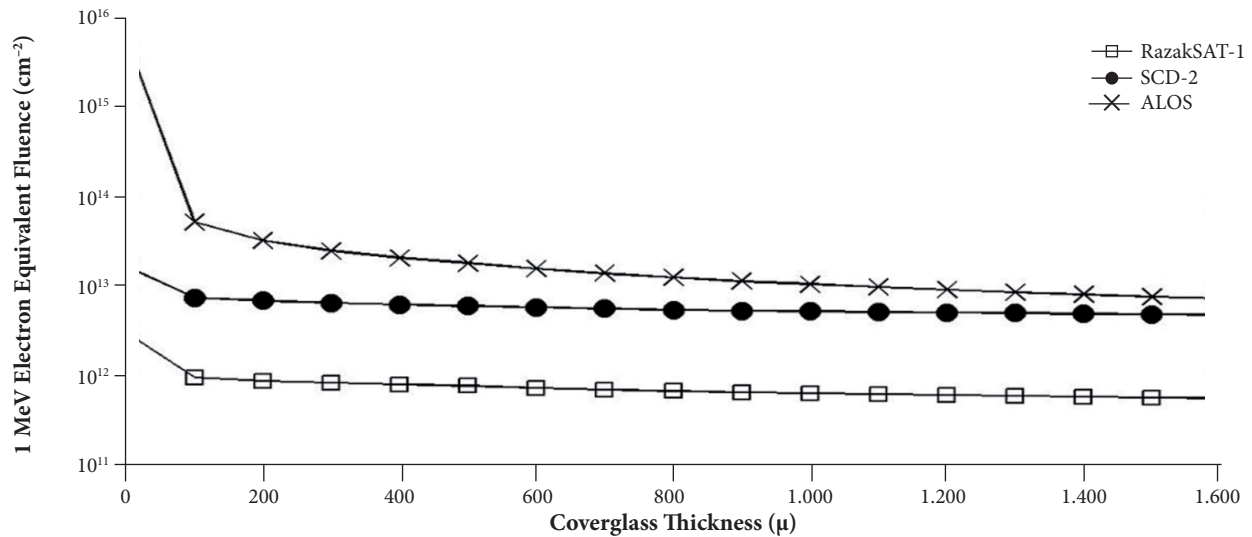
Figure 6. Effective dose of 1 MeV electrons towards the GaAs solar cell as a function of the shielding thickness over three years for three satellite orbits.
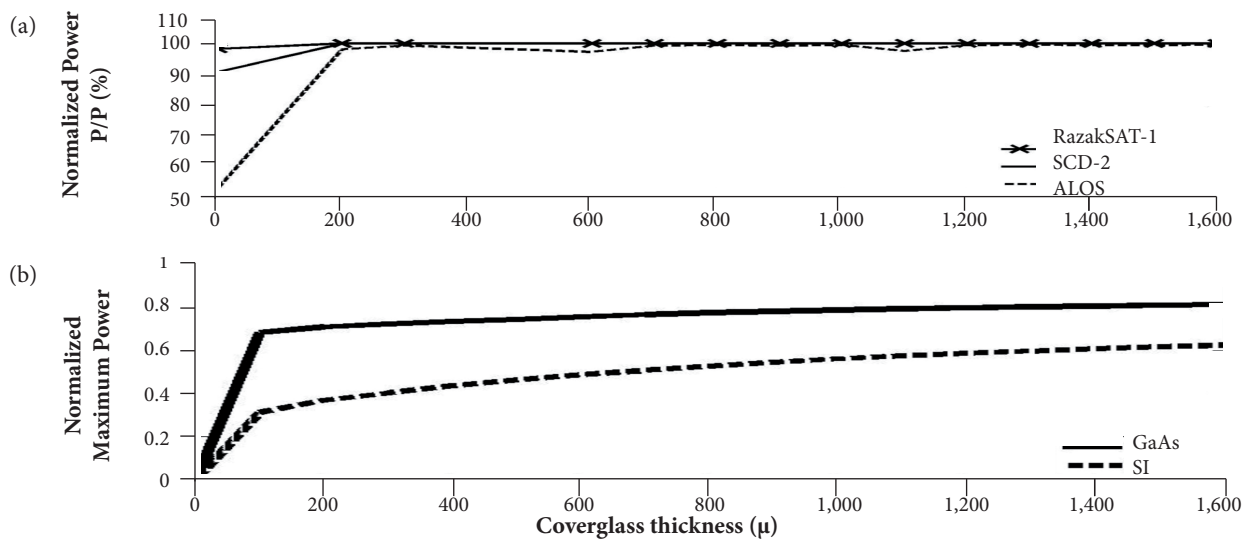

Figure 7. Normalized maximum power of (a) GaAs solar cells at various orbits and (b) two solar-cell materials in the RazakSAT-1 orbit over three years.

increasing the cover-glass thickness. By using the GaAs material is expected to increase the power of the solar cell by approximately 29% more than the Si material when it is shielded with 0.5 mm of silica glass. Hence, GaAs was used in RazakSAT-1 to provide higher resistance to radiation damage in orbit.

GEOMAGNETIC CONDITION ANALYSIS

The geomagnetic conditions when communication of RazakSAT-1 disrupted are shown in Fig. 8. The geomagnetic conditions were described using the K_p and *Dst* indices and were compared with the trapped particle fluxes of three NOAA satellites for three months (June, July, and August, 2010). The figure indicates that the three NOAA satellites had similar flux trends, and all the three satellites detected sudden peak fluxes on August 4, 2010. At this point, the K_p value was 4, and the

Dst index was –49 nT. Although the values may indicate possible degradation of the high-frequency band, the geomagnetic conditions for the entire three months are mild and insufficient to cause permanent damage to the communication devices. In addition, Table 5 simplifies the relationship between the geomagnetic disturbances and the trapped particle fluxes of the three NOAA satellites. The geomagnetic disturbances are found to be moderately consistent with the trapped-particle fluxes of all three NOAA satellites.

Apart from the data of the NOAA/POES satellites and geomagnetic indices, Fig. 9 demonstrates the monthly fluxes of the GCR and trapped particles in the RazakSAT-1 orbit, which estimated by the SPENVIS models from July 14, 2009 to July 14, 2012. Based on this figure, the GCR fluxes remain anti-correlated with the trapped particle fluxes, whereas the SPENVIS models did not estimate any sudden anomalies over the three years. Thus, the NOAA/POES and geomagnetic source observations and the model data showed that the space radiation calculated on average in the orbit may not be responsible for the uncompleted mission of RazakSAT-1. In other words, the models considered fluxes and doses for the whole orbit. Hence, this suggests that the satellite may experience anomalies in a specific region, such as the SAA region, where the LEO-NEqO satellites revisited more frequently. In addition, the doses received by the satellite from the SAA alone might need to be studied further in order to evaluate the major influence of space particles toward the LEO/NEqO satellites.
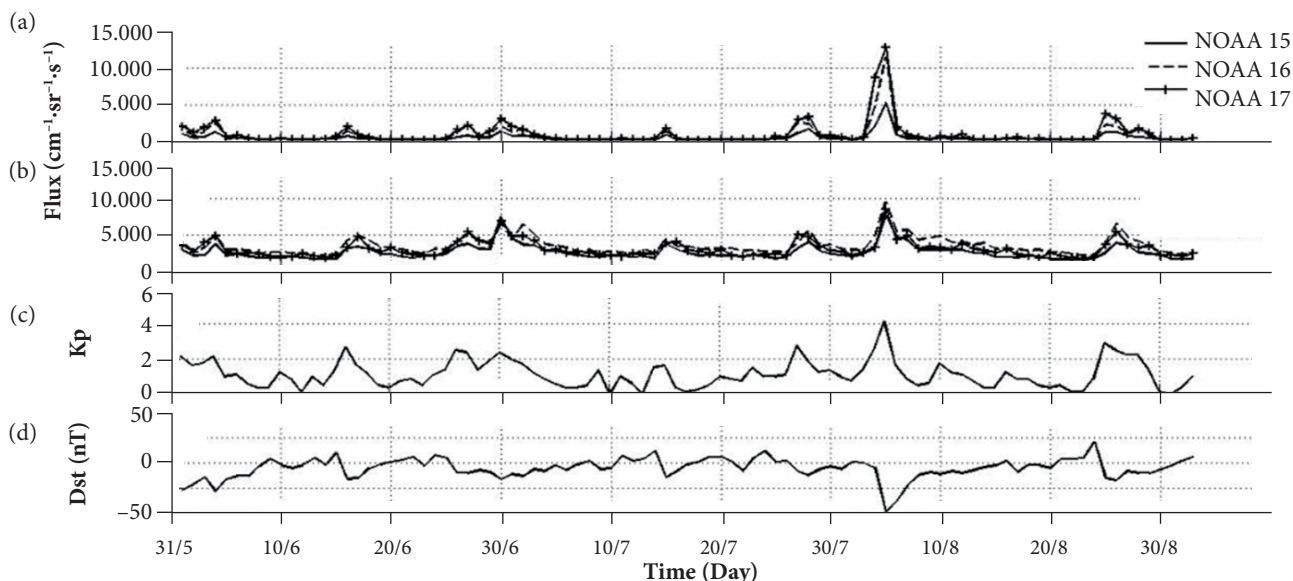

Figure 8. Comparison of (a) trapped protons and (b) trapped electrons fluxes obtained from three NOAA/POES satellites with geomagnetic conditions following (c) the Kp index and (d) the Dst index from June to August, 2010 when communication with RazakSAT-1 was likely lost. The geomagnetic data was obtained from NOAA (2016).

Table 5. Relationship between trapped particles with Kp and Dst indices for three NOAA satellites.

Particle	Satellite	Correlation Coefficient	
		K_p	*Dst*
Trapped Protons	NOAA-15	0.7275	–0.6422
	NOAA-16	0.7335	–0.6350
	NOAA-17	0.7480	–0.5968
Trapped Electrons	NOAA-15	0.6654	–0.7114
	NOAA-16	0.6844	–0.7346
	NOAA-17	0.7211	–0.7125

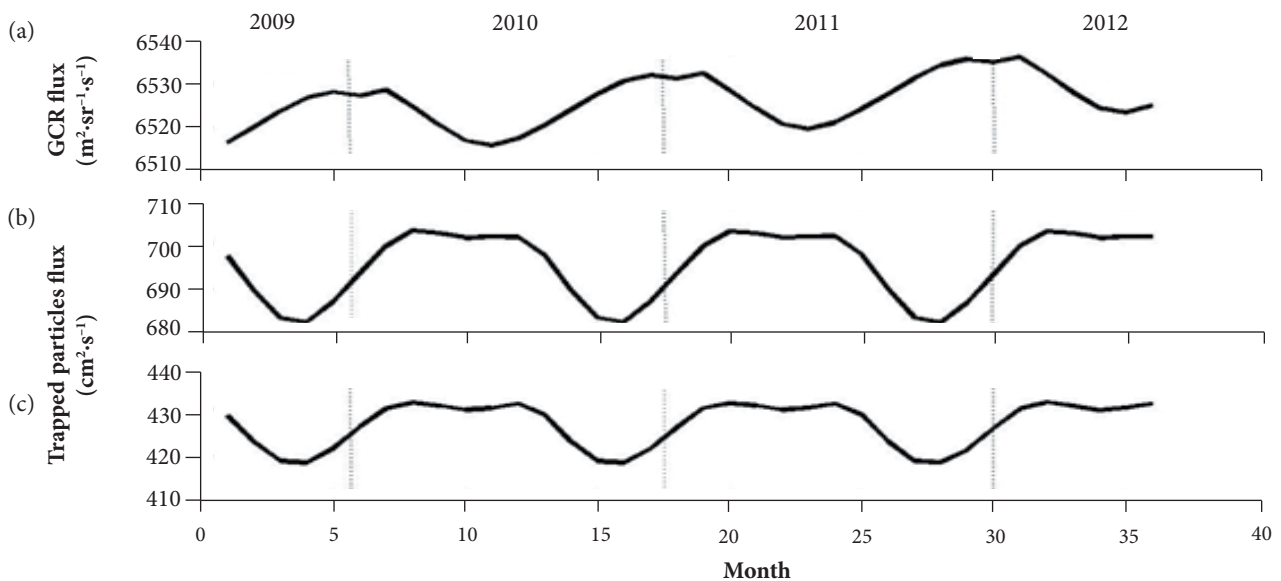**Figure 9.** Estimated monthly fluxes of (a) GCR, (b) trapped protons and (c) trapped electrons for RazakSAT-1 from July 14, 2009 to July 14, 2012.

SUMMARY AND CONCLUSION

The radiation environment in the LEO/NEqO of the RazakSAT-1 was assessed through the fluxes of three space radiation sources: GCR, SEPs, and trapped particles. The fluxes of GCR, SEPs, trapped protons and trapped electrons were predicted using the CREME96, ESP-PSYCHIC, AP-8 and AE-8 models, respectively. GCR dominated the LEO/NEqO in the high-energy range of 10^3 to 10^4 MeV, and no SEPs were detected because the shielding works very effectively in LEO/NEqO. The maximum GCR flux in the LEO/NEqO was approximately 16.23 times less than the fluxes in the polar orbit. The fluxes of trapped protons and trapped electrons in the NEqO were 1 and 10 times less, respectively, than those in the polar orbit.

In terms of the radiation dose comparison, the maximum LET values for RazakSAT-1 was 1087 MeV $cm^2 g^{-1}$, and it is almost similar with SCD-2, and two times lower compared to ALOS. RazakSAT-1 is estimated to experience 1 to 10 and 3 to 120 times less of LET damage compared to SCD and ALOS, respectively. The ionization that occurred in all three satellites is mainly attributed by protons, which produce greater nuclear interactions. RazakSAT-1 has the lowest SEU rates, compared to those of SCD-2 and ALOS. In addition to the radiation dose, RazakSAT-1, with 5 mm Al shielding, has the lowest estimated TID of approximately 1 and 15 times less than the TID of SCD-2 and ALOS, respectively. For solar cells, 0.01 mm of silica glass can improve the performance of satellites in the orbit by 0.05% for RazakSAT-1, 0.40% for SCD-2, and 2.19% for ALOS. In other words, the GaAs material that was used in RazakSAT-1, with 0.5 mm silica glass, also provides 29% better radiation resistance than the Si.

The environmental data from NOAA-15, 16, and 17 satellites and the geomagnetic indices over the expected period of disruption (three-month) showed that mild conditions were obtained, except for a sudden peak of geomagnetic activity on August 4, 2010. However, this event was insufficient to cause sudden damage to the communication frequency band of RazakSAT-1. The estimated monthly fluxes of GCR and trapped particles from the SPENVIS models do not show any anomalies during the three-year mission of RazakSAT-1, which implies that the space radiation environment is not a factor that causes loss of communication in RazakSAT-1. The models also consider average fluxes and doses received throughout the orbit. Thus, the dose received by satellites from SAA should be performed in more detail to evaluate the accuracy of risk in LEO/NEqO. For the case of RazakSAT-1, the material stored beyond the time limits required (waiting to launch), it may be one of the factors degrading the performance of the satellite. In addition to the space radiation environment, other factors also need to be investigated to understand what had happened during the RazakSAT-1 mission.

ACKNOWLEDGMENTS

AUTHOR'S CONTRIBUTION

Conceptualization, Suparta W; Methodology, Suparta W and Zulkeple SK; Investigation, Suparta W and Zulkeple SK; Writing – Original Draft, Suparta W and Zulkeple SK; Writing – Review and Editing, Suparta W; Funding Acquisition, Suparta W; Resources, Suparta W and Zulkeple SK; Supervision, Suparta W.

REFERENCES

Adams Jr. JH (1986) Cosmic ray effects on microelectronics, Part IV (Report 5901). NRL Memorandum Reports.

Ahmad A (2013) Classification simulation of RazakSAT satellite. Procedia Engineering 53:472-482. doi: 10.1016/j.proeng.2013.02.061

Barkas WH, Berger MJ (1964) Tables of energy losses and ranges of heavy charged particles (Report SP-3013). NASA Technical Report.

Benton ER, Benton EV (2001) Space radiation dosimetry in low-Earth orbit and beyond. Nuclear Instruments and Methods in Physics Research B 184(1-2):255-294. doi: 10.1016/S0168-583X(01)00748-0

Chun HJ, Kim BJ, Chang HS, Kim EE, Park WK, Park SD, Ashard A (2006) RazakSAT – a high performance satellite waiting for its mission in space. Presented at: 20th Annual AIAA/USU Conference on Small Satellites. Proceedings of the AIAA/USU Conference on Small Satellites, Session IV, SSC06-VI-6.

Hashim M, El-Mahallawy MS, Reba MNM, Abas AA, Ahmad S, Yap XQ, Marghany M, Arshad AS (2013) Geometric and radiometric evaluation of RazakSAT medium-sized aperture camera data. International Journal of Remote Sensing 34(11):3947-3967. doi: 10.1080/01431161.2013.770581

Heynderickx D, Quaghebeur B, Wera J, Daly EJ, Evans HDR (2004) New radiation environment and effects models in the European Space Agency's Space Environment Information System (SPENVIS). Space Weather 2(10). doi: 10.1029/2004SW000073

Lawal AD, Radice GM (2013) Near equatorial orbit small SAR constellation for developing nations. International Journal of Research in Engineering and Technology 2(4):654-651.

Messenger SR, Walters RJ, Warner JH, Evans H, Taylor SJ, Baur C, Heynderickx D (2008) Status of implementation of displacement damage dose method for space solar cell degradation analyses. Proceedings of the 8th European Space Power Conference, 2008; Constance, Germany.

Murtaza, H (2011) Prediction of the space radiation environment of PakSat, a geostationary communication satellite. Journal of Space Technology 1(1):73-77.

NOAA (2016) ftp://ftp.ngdc.noaa.gov/STP/GEOMAGNETIC_DATA/INDICES/

Rodger CJ, Clilverd MA, Green JC, Lam MM (2010) Use of POES SEM-2 observations to examine radiation belt dynamics and energetic electron precipitation into the atmosphere. J. Geophys. Res. 115(A4). doi: 10.1029 /2008JA014023

Samwel SW, Hady AA (2009) Space radiation environment forecast for EGYPTSAT-2 satellite. Space Weather 7(12). doi: 10.1029/2009SW000482

Sawyer DM, Vette JI (1976) AP-8 Trapped proton environment for solar maximum and solar minimum (NSSDC/WDC-A-R/S, 76-06). NASA Technical Report.

Seltzer SM (1994) Updated calculations for routine space-shielding radiation dose estimates: SHIELDOSE-2 (NISTIR, 5477). NIST Pubs.

Tada HY, Carter Jr. JR, Anspaugh BE, Downing RG (1982) Solar cell radiation handbook. 3rd ed. California: JPL Publication.

Vette JI (1991) The AE-8 trapped electron model environment (NSSDC/WDC-A-RS-91-24). NASA Technical Report.

Xapsos MA, Stauffer C, Jordan T, Barth JL, Mewaldt RA (2007) Model for cumulative solar heavy ion energy and linear energy transfer spectra. IEEE Transaction Nuclear Science 54(6):1985-1989. doi: 10.1109/TNS.2007.910850